Jurnal Teknologi

Dumbbell Shaped Inline Mach–Zehnder Interferometer for Bio-Chemical detection

A. Lokman[a], H. Arof[a], N. M. Ali[a], S. W. Harun[a,b*]

[a]Department of Electrical Engineering, Faculty of Engineering, University of Malaya, 50603, Kuala Lumpur, Malaysia
[b]Photonics Research Center, University of Malaya, 50603, Kuala Lumpur, Malaysia

Graphical abstract
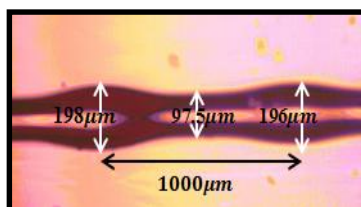
Abstract

A new dumbbell-shaped inline Mach Zehnder interferometer (MZI) is developed using an arcing process of a fusion splicer for measurement of various bio-chemical concentrations in distilled water. The sensor probe consists of two bulges separated by a tapered waist that generates a good reflected interference spectrum. The interference spectrum is red-shifted with the increase in the bio-chemical concentration due to the increment of the refractive index of the surrounding medium, which reduces the phase difference between the core and cladding modes. In sensing the concentration of glucose solution from 0% to 12%, the dip wavelength increases from 1554.419 to 1554.939 nm in a quadratic manner with the coefficient of determination of 0.9818. The sensor has a sensitivity of 0.0354nm/%. The corresponding linearity is 99.05% and the limit of detection is 3.87%. For NaCl solution, the shift in dip-wavelength is linearly proportional to the increase in its concentration. The sensitivity obtained is 0.0329 nm/% with a linearity of more than 99.68%. The limit of detection is 4.32%. Lastly, for uric acid solution, the sensitivity obtained is 0.0006 nm/%. The slope shows a good linearity of more than 99.48% for a 7.52% limit of detection.

Keywords: Inline Mach Zehnder Interferometer (MZI), fiber sensor, Dumbell-shape structure; refractive index; glucose

Abstrak

Interferometer Mach Zehnder (MZI) berbentuk baris baru Dumbbell dibangunkan menggunakan proses pengarkaan daripada spliser gabungan untuk mengukur kepekatan pelbagai bio-kimia di dalam air suling. Probe sensor terdiri daripada dua bonjolan dipisahkan oleh pinggang tirus yang menjana baik yang mencerminkan spektrum gangguan. Spektrum gangguan adalah merah-beralih dengan peningkatan dalam kepekatan bio-kimia disebabkan oleh kenaikan indeks biasan sederhana sekitarnya, yang mengurangkan perbezaan fasa antara mod teras dan pelapisan. Dalam penderiaan kepekatan larutan glukosa dari 0% hingga 12%, yang berenang panjang gelombang kenaikan 1554,419-1554,939 nm secara kuadratik dengan pekali penentuan 0,9818. Sensor ini mempunyai sensitiviti 0.0354 nm /%. The kelinearan sama adalah 99,05% dan had pengesanan adalah 3.87%. Untuk penyelesaian NaCl, peralihan dalam kemiringan panjang gelombang adalah berkadar linear kepada peningkatan dalam kepekatan. Kepekaan diperolehi adalah 0,0329 nm /% dengan kelinearan lebih daripada 99.68%. Had pengesanan adalah 4.32%. Akhir sekali, untuk penyelesaian urik asid, kepekaan yang diperolehi adalah 0,0006 nm /%. Cerun menunjukkan kelinearan yang baik lebih daripada 99,48% bagi had 7.52% daripada pengesanan.

Kata kunci: Inline Mach Zehnder Interferometer (MZI), Sensor gentian, struktur bentuk Dumbbell, indeks biasan, glukosa

1.0 INTRODUCTION

Abnormal levels of glucose, sodium and uric acid in human serum and urine are related to several medical complications such as diabetes, high blood pressure, gout, dysfunctional kidney and cardiovascular diseases. Conventional methods that have been developed to detect the levels of these bio-chemicals in human body include liquid chromatography (HPLC) [1-3], enzymatic assay [4-6] and other electrochemical [7, 8] processes. Of late, optical fiber sensors have also been used to detect physical parameters as well as chemical compounds [9]. Optical fiber sensors offer many advantages since they are compact, highly sensitive, immune to electromagnetic interference, resistant to corrosion and placid to volatile surrounding.

Optical fiber Mach–Zehnder interferometer (MZI) has been widely used as a probe for various sensing applications. For instance, inline fiber MZI sensors have been utilized for monitoring changes in refractive index, strain and temperature. In the last ten years, many designs have been proposed for constructing MZI sensors using tapered fibers [10], long-period gratings (LPGs) [11, 12], two different single-mode fibers (SMFs) [13, 14] and some other special configurations [15-17].

In this paper, a simpler inline MZI with a dumbbell-shaped structure is proposed for detecting various bio-chemicals such as glucose, sodium and uric acid in distilled water. The proposed MZI structure comprises two bulges connected by a tapered waist. Compared to intensity-based sensors, the proposed sensor is more reliable and practical since it is based on wavelength shift. It shows a high potential for bio-chemical sensing as it has fast response, low fabrication cost and compact size.

2.0 EXPERIMENTAL

To fabricate the MZI structure, a single mode fiber (SMF) is cleaved into two sections, each with a flat and smooth end-surface, as illustrated in Figure 1 (a). Then the end facets of the two sections are linked and fused using the manual "arc" function of a commercial fusion splicer (Sumitomo Type 39). The fusion splicer heats the ends of the two fiber sections to soften them before exerting pressure from both sides to merge and fuse them back into a single fiber. The "arc" function is used repeatedly for a few times to lump more silica at the joint thus forming the first bulge as shown in Figure 1(b). Once the first bulge is formed, the jointed fiber is then cleaved again at 1 mm away from the center of the first bulge as illustrated in Figure 1(c). Again, the cleaved fiber sections are fused using the "arc" function in a similar fashion as before to form the second bulge. The two bulges are separated by a thinner waist area. The completed dumbbell structure is shown in Figure 2 where the diameters of the first and second bulges are 198 μm and 196 μm respectively. The diameter of the waist section is about 97.5 μm and its length is approximately 1000 μm while the length of the whole structure is around 2000 μm.
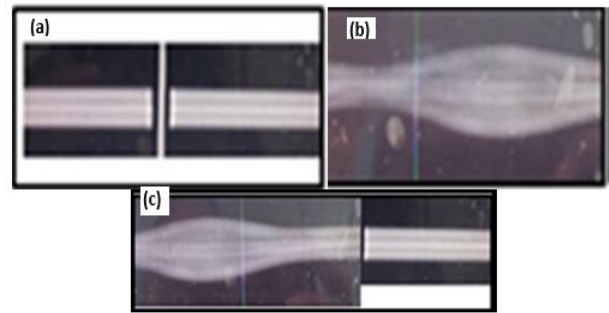
Figure 1 Fabrication steps of the dumbbell shaped MZI (a) Two sections SMF with cleaved end surface (b) Formation of first bulge (c) The second bulge is formed in a similar fashion
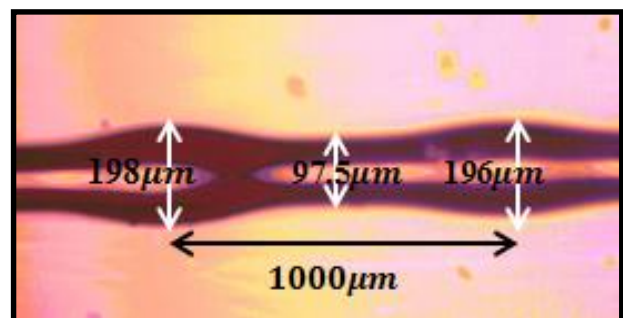
Figure 2 The microscope image of the fabricated dumbbell shaped MZI

Figure 3 shows the experimental setup of the bio-chemical sensing using a dumbbell-shaped MZI probe. The input signal from an amplified spontaneous emission (ASE) laser source is launched into the sensor probe via a 3 dB coupler. The reflected signal from the sensor is then routed into an optical spectrum analyzer (OSA) through the same coupler. When the input single mode light beam reaches the first bulge of the sensor probe, it is divided into two parts where the first part continues to propagate in the core, while the other part travels in the cladding of the SMF. Due to the optical path difference (OPD) between the core and cladding mode, an interference pattern is established when the two output beams recombine at the output end of the second bulge. The interference pattern is strongly dependent on the refractive index of the surrounding medium.
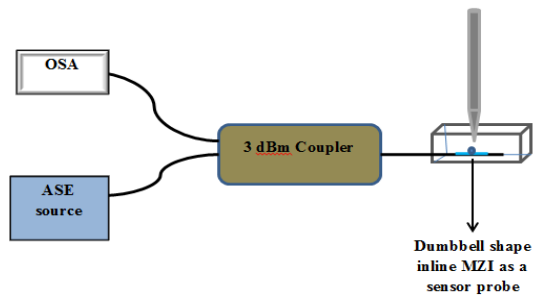
Figure 3 The experimental setup of the proposed biochemical sensors

3.0 RESULTS AND DISCUSSION

First, glucose solution of different concentrations were prepared by mixing glucose and distilled water, and their refractive indices were measured. The refractive indices of this solution were 1.333, 1.336, 1.339, 1.3425, 1.3461, 1.3494 and 1.353 at glucose concentrations of 0 %, 2 %, 4 %, 8 %, 10 % and 12 %, respectively. Due to the compact structure of the sensor, a single drop of the liquid solution was enough to surround the whole dumbbell structure. The reflected spectrum from the MZI covered in the glucose solution was then measured. After each measurement, the MZI was cleansed with deionized water and compressed air. Figure 4 shows the reflected interference spectrum of the output for different glucose concentrations. It could be seen that the wavelength is red-shifted with the increase of the surrounding glucose concentration from 0 % to 12 %. This is due to the phase difference between the core and cladding mode, which reduces when the refractive index of the surrounding medium increases. The unsmooth curve shows the variation of the surface roughness of the tapered waist, which results in the non-uniqueness of the cladding modes. While the inline MZI is placed in glucose solution, the difference in refractive index of the cladding and glucose solution is big enough to support several cladding modes in the dumbbell structure. All the non-uniqueness cladding modes interfere with the core mode while oscillating inside the dumbbell structure.
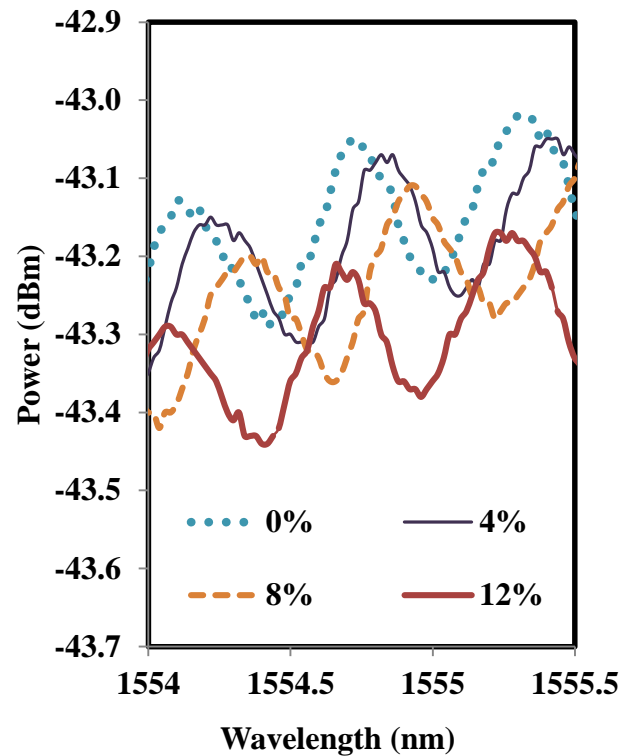
Figure 4 Reflected spectrum from the dumbbell shape MZI immersed into various glucose concentrations

The change in the transmission dip wavelength with the increase in glucose concentration is depicted in Figure 5. The wavelength increases in a quadratic manner with the increase in glucose concentration. The adjusted R-square value or the coefficient of determination is the measure of the goodness of fit which is 0.9818. The considerably high value of the adjusted R-square allows the prediction of unknown concentration by the model. As the glucose concentration increases from 0 to 12%, the dip wavelength increases from 1554.419 to 1554.939 nm. A linear trend line is also added in the graph representing the relation between one of the the dip wavelengths of the interference spectrum and the glucose concentration as shown in the inset of Figure 5. It is found that the sensor has a sensitivity of 0.0275 nm/% with a linearity of 99.78% and limit of detection of 3.87%. The value of limit of detection is obtained by dividing the standard deviation with the sensitivity of the sensor.
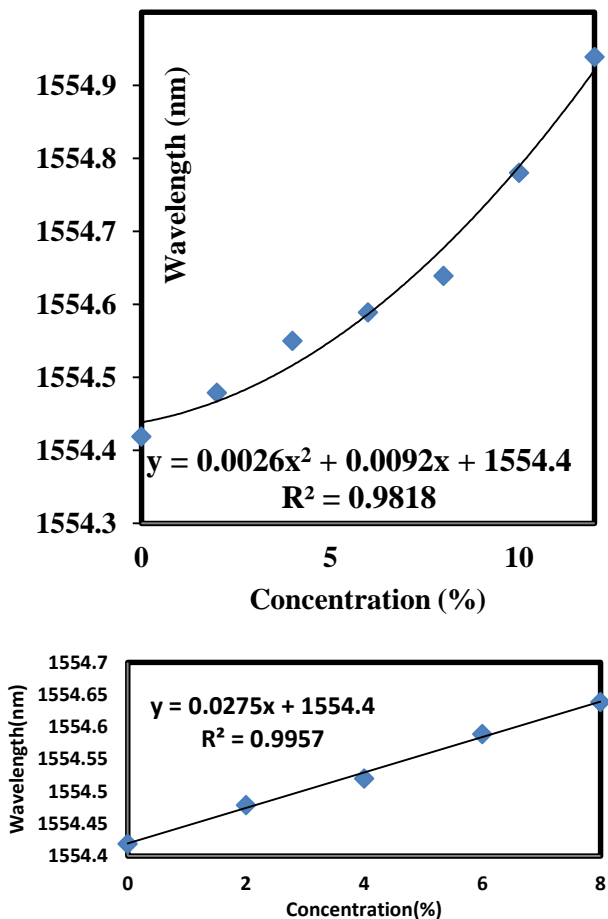
Figure 5 The relation between one of the measured dip wavelengths of the interference spectrum and the glucose concentration in distilled water

The experiment is then repeated on Sodium Chloride (NaCl) solution with different proportions ranging from 0% to 12%. The refractive indices of this solution were 1.3325, 1.33511, 13382, 1.341, 1.3441, 1.3469, and 1.3499 at NaCl concentrations of 0 %, 2 %, 4 %, 8 %, 10 % and 12 %, respectively. Figure 6 shows the reflected output spectrum from the MZI at various NaCl concentrations. From the experimental results it is seen that an increase in NaCl concentration can be detected by observing the shift of the interference spectrum of the reflected light. A higher concentration of NaCl solution corresponds to a higher refractive index and thus the transmission peak/dip of the spectrum is red-shifted. Higher refractive index reduces the phase difference between the core and cladding mode resulting in a shift in the free-spectral range of the interference spectrum and subsequently increasing the transmission peak or dip wavelength of the comb spectrum.

Figure 7 shows the operating wavelength of one of the transmission dips for the comb spectrum against different sodium chloride concentration measured from the light reflected of the MZI. The sensitivity is obtained at 0.033 nm/% and the slope shows a good linearity of more than 99% for a 4.32% limit of detection. The results indicate a linear relationship between the signals reflected from the MZI as a function of the concentration of the sodium chloride. We may conclude that an increase in sodium chloride concentration can be detected by observing the shift in the comb spectrum due to the change of medium's refractive index, which increases as its concentration rises.

Lastly, the experiment was repeated with uric acid with its concentration ranging from 0 to 500 ppm. The refractive indices of this solution were 1.333, 1.3331, 1.3332, 1.3334, 1.3335 and 1.3336 at uric acid concentrations of 0 ppm, 100 ppm, 200 ppm, 300 ppm, 400 ppm and 500 ppm respectively. Figure 8 shows the output comb spectrum of the sensor at various urid acid concentrations in DI water solution. As expected, the interference spectrum of the output is also red-shifted when the concentration of uric acid rises from 0 to 500 ppm. The wavelength change of one of the transmission dips with the increase in uric acid concentration is depicted in Figure 9. As observed, the dip-wavelength shift linearly increases as the concentration of the uric acid of the solution increases. The sensitivity is obtained at 0.0006 nm/% and the slope shows a good linearity of more than 99.48% for a 7.52% limit of detection.
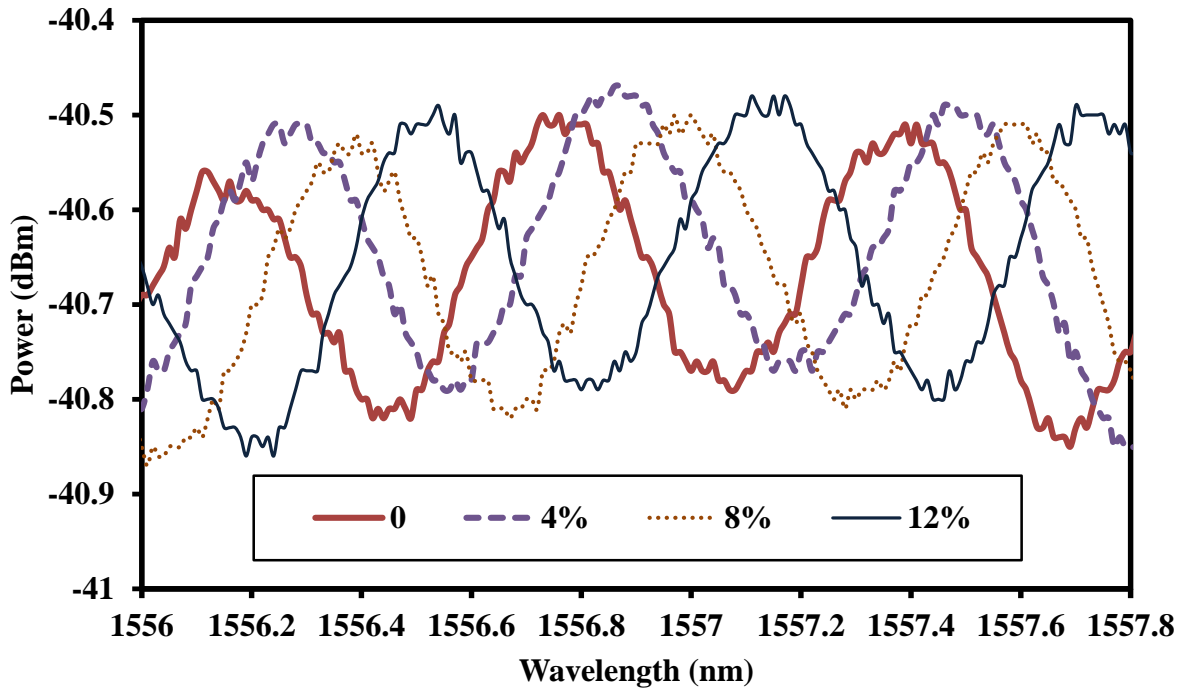
Figure 6 The measured dip wavelength of the interference spectrum against the sodium chloride concentration in distilled water

$y = 0.0329x + 1557$
$R^2 = 0.9937$
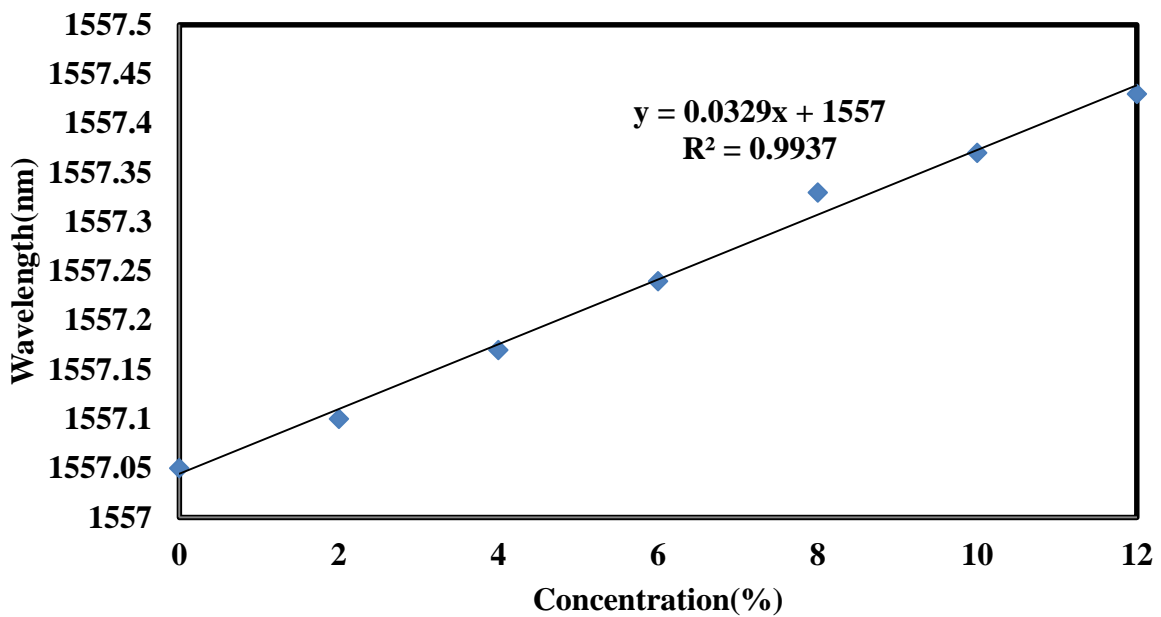
Figure 7 The measured dip wavelength of the interference spectrum against the glucose concentration in distilled water
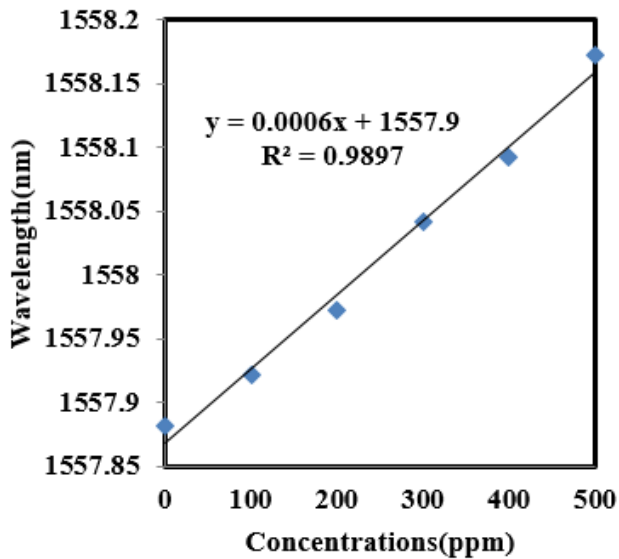
Figure 8 The output comb spectrum of the sensor at various urid acid concentrations in DI water solution

The sensor performance is then summarized in Table 1. Overall, the sensor is observed to be sufficiently stable with a standard deviation ranging from 3.87 to 7.52 % with a linearity of more than 99%. Throughout the experiment, a fixed quantity of liquid solution was placed in the petri dish and the corresponding dip wavelength was measured by using an OSA. The results show that the proposed sensor is applicable and useful for bio-chemical detection due to its ability to provide real time bio-chemical detection and control of various mixtures continuously. This preliminary result shows that the proposed dumbbell shaped MZI probe can be used as a refractive index sensor.

Table 1 Performance of bio-chemical sensors

Parameter	Glucose	NaCl	Uric Acid
Sensitivity	0.0275%	0.0329	0.0006
Linear Range	0-12%	0-12%	0-500ppm
Linearity	99.98%	99.68%	99.48%
Limit of Detection	3.87%	4.32%	7.52%
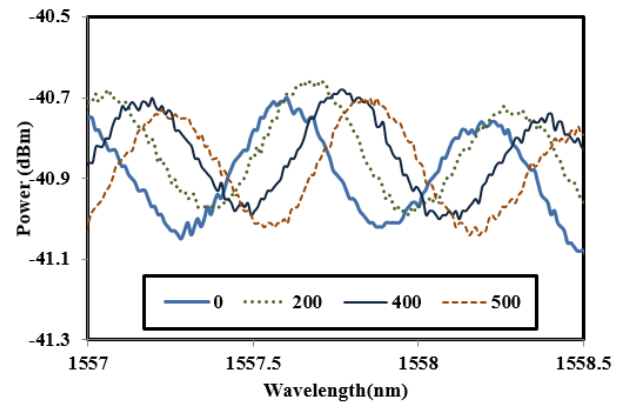
Figure 9 The wavelength change of one of the transmission dips with the increase in uric acid concentration

4.0 CONCLUSION

A new dumbbell-shaped inline MZI is developed using an arcing process of a fusion splicer for bio-chemical detection in distilled water. The sensor probe consists of two bulges separated by a tapered waist that generates a good reflected interference spectrum. The interference spectrum is red-shifted with the increase of bio-chemical concentration due to the increase of the refractive index of the surrounding, which reduces the phase difference between the core and cladding modes. As the glucose concentration increases from 0 to 12%, the dip wavelength red-shifts from 1554.419 to 1554.939 nm in a quadratic manner with the coefficient of determination of 0.9818. It is also found that the sensor has a sensitivity of 0.0354nm/% with a linearity of 99.05% and limit of detection 3.87%. For NaCl solution, the dip-wavelength shift is linearly proportional to the increase of the concentration of the sodium chloride solution or its salinity. The sensitivity is obtained at 0.0329 nm/% and the slope shows a good linearity of more than 99.68% for a 4.32% limit of detection. Lastly, for uric acid, the sensitivity is obtained at 0.0006 nm/% and the slope shows a good linearity of more than 99.48% for a 7.52% limit of detection.

References

[1] Zhao, C. L., Yang, X., Demokan, M. S., & Jin, W. 2006. Simultaneous Temperature and Refractive Index Measurements Using a 3 Slanted Multimode Fiber Bragg Grating. *Journal of Lightwave Technology*. 24(2): 879.
[2] Shu, X., Gwandu, B. A., Liu, Y., Zhang, L., & Bennion, I. 2001. Sampled Fiber Bragg Grating for Simultaneous Refractive-Index and Temperature Measurement. *Optics Letters*. 26(11): 774-776.

[3]   Gwandu, B. A., Shu, X., Allsop, T. D., Zhang, W., Zhang, L., Webb, D. J., & Bennion, I. 2002. Simultaneous Refractive Index and Temperature Measurement Using Cascaded Long-period Grating in Double-Cladding Fibre. *Electronics Letters*. 38(14): 695-696.

[4]   Tian, Z., Yam, S. H., & Loock, H. P. 2008. Single-mode Fiber Refractive Index Sensor Based On Core-Offset Attenuators. *Photonics Technology Letters, IEEE*. 20(16): 1387-1389.

[5]   Wang, Y., Yang, M., Wang, D. N., Liu, S., & Lu, P. 2010. Fiber in-line Mach-Zehnder Interferometer Fabricated by Femtosecond Laser Micromachining for Refractive Index Measurement with High Sensitivity. *JOSA B*. 27(3): 370-374.

[6]   Jiang, L., Zhao, L., Wang, S., Yang, J., & Xiao, H. 2011. Femtosecond Laser Fabricated All-Optical Fiber Sensors with Ultrahigh Refractive Index Sensitivity: Modeling and Experiment. *Optics Express*. 19(18): 17591-17598.

[7]   Zhu, T., Wu, D., Deng, M., Duan, D., Rao, Y., & Bao, X. 2011. Refractive Index Sensing Based on Mach-Zehnder Interferometer Formed by Three Cascaded Single-mode Fiber Tapers. In *21st International Conference on Optical Fibre Sensors (OFS21)* International Society for Optics and Photonics. 77532P-77532P.

[8]   Villatoro, J., Monzón-Hernández, D., & Talavera, D. 2004. High Resolution Refractive Index Sensing with Cladded Multimode Tapered Optical Fibre. *Electronics Letters*. 40(2): 106-107.

[9]   Kieu, K. Q., & Mansuripur, M. 2006. Biconical Fiber Taper Sensors. *Photonics Technology Letters, IEEE*. 18(21): 2239-2241.

[10] Wu, D., Zhu, T., Deng, M., Duan, D. W., Shi, L. L., Yao, J., & Rao, Y. J. 2011. Refractive Index Sensing Based on Mach–Zehnder Interferometer Formed by Three Cascaded Single-Mode Fiber Tapers. *Applied Optics*. 50(11): 1548-1553.

[11] Patrick, H. J., Kersey, A. D., & Bucholtz, F. 1998. Analysis of the Response of Long Period Fiber Gratings to External Index of Refraction. *Journal of Lightwave Technology*. 16(9): 1606.

[12] Chiang, K. S., Liu, Y., Ng, M. N., & Dong, X. 2000. Analysis of Etched Long-Period Fibre Grating and Its Response to External Refractive Index. *Electronics Letters*. 36(11): 966-967.

[13] Wu, Q., Semenova, Y., Wang, P., & Farrell, G. 2011. High Sensitivity SMS Fiber Structure Based Refractometer– Analysis and Experiment. *Optics Express*. 19(9): 7937-7944.

[14] Cárdenas-Sevilla, G. A., Fávero, F. C., & Villatoro, J. 2013. High-Visibility Photonic Crystal Fiber Interferometer as Multifunctional Sensor. *Sensors*. 13(2): 2349-2358.

[15] Wu, D., Zhu, T., Chiang, K. S., & Deng, M. 2012. All Single-Mode Fiber Mach–Zehnder Interferometer Based on Two Peanut-Shape Structures. *Journal of Lightwave Technology*. 30(5): 805-810.

[16] Yang, R., Yu, Y. S., Xue, Y., Chen, C., Chen, Q. D., & Sun, H. B. 2011. Single S-tapered fiber Mach–Zehnder interferometers. *Optics Letters*. 36(23): 4482-4484.

[17] Jasim, A. A., Harun, S. W., Arof, H., & Ahmad, H. 2013. Inline Microfiber Mach–Zehnder Interferometer for High Temperature Sensing.